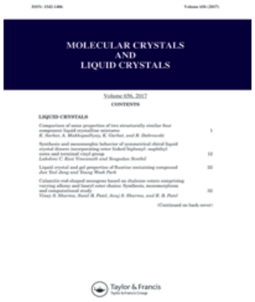

Taylor & Francis
Taylor & Francis Group

Molecular Crystals and Liquid Crystals

ISSN: 1542-1406 (Print) 1563-5287 (Online) Journal homepage: http://www.tandfonline.com/loi/gmcl20

Calamitic-rod-shaped mesogens based on chalcone esters comprising varying alkoxy and lauryl ester chains: Synthesis, mesomorphism and computational study

Vinay S. Sharma, Sunil B. Patel, Anuj S. Sharma & R. B. Patel

To cite this article: Vinay S. Sharma, Sunil B. Patel, Anuj S. Sharma & R. B. Patel (2017) Calamitic-rod-shaped mesogens based on chalcone esters comprising varying alkoxy and lauryl ester chains: Synthesis, mesomorphism and computational study, Molecular Crystals and Liquid Crystals, 656:1, 32-47, DOI: 10.1080/15421406.2017.1393167

To link to this article: https://doi.org/10.1080/15421406.2017.1393167

MOLECULAR CRYSTALS AND LIQUID CRYSTALS
2017, VOL. 656, 32–47
https://doi.org/10.1080/15421406.2017.1393167

Calamitic-rod-shaped mesogens based on chalcone esters comprising varying alkoxy and lauryl ester chains: Synthesis, mesomorphism and computational study

Vinay S. Sharma[a], Sunil B. Patel[b], Anuj S. Sharma[b], and R. B. Patel[a]

[a]Chemistry Department, K. K. Shah Jarodwala Maninagar Science College, Gujarat University, Ahmedabad, Gujarat, India; [b]Department of Chemistry, School of Science, Gujarat University, Ahmedabad, Gujarat, India

ABSTRACT
In this study we have synthesized a new class of compounds incorporating of chalconyl-ester and terminally substituted lauryl group. A series of new chalcones with three aromatic rings is synthesized and characterised by elemental analyses and spectroscopic techniques such as Fourier transform infrared [FT-IR] and proton magnetic resonance magnetic resonance [^{1}H NMR] spectroscopy. The mesomorphic properties of these compounds were observed by optical polarized light microscopy (POM) and confirmed by differential scanning calorimetry (DSC). It is found that all the prepared materials display enantiotropic LCs phases except first two homologue in present series. The lower member comp. (C_3 to C_6) display only SmC phase while comp. (C_7 to C_{12}) shows smectic C as well as nematic phase. The higher member comp. (C_{14} to C_{18}) display only nematic phase in heating and cooling condition. To get more insights, the HOMO, LUMO studies are carried out which supports intramolecular charge transfer interactions in this class of mesogens.

KEYWORDS
Chalcone; lauryl ester; mesomorphic; nematic; smectic

GRAPHICAL ABSTRACT

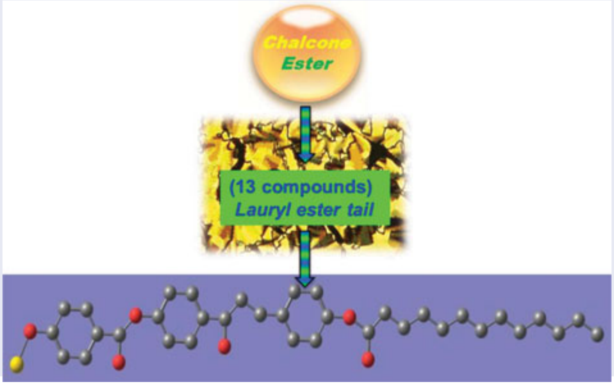

1. Introduction

Thermotropic liquid crystals are an important class of self-organized molecular entities which are in dynamic motion yet possessing long range orientational order [1–2]. Thermotropic LC

CONTACT Vinay S. Sharma ✉ vinaysharma3836@gmail.com Chemistry Department, K.K. Shah Jarodwala Maninagar Science College, Gujarat University, Ahmedabad, Gujarat, 380008, India.
Color versions of one or more of the figures in the article can be found online at www.tandfonline.com/gmcl.

molecule consists a core, which is usually a linker rod like linked aromatic ring by different linker unit and tail part which are either straight alkyl or alkoxy chains whose terminal unit is obviously a polar substituent to providing flexibility to stabilize the molecular alignment. Base on the type of the substituents and their combinations, both nematic and smectic mesophases may be formed [3–5]. Study of liquid crystalline state is a multidisciplinary subject and useful to mankind and various industrial applications [6–9] due to its unique property to flow as liquid and optical properties as crystals. The construction of liquid crystalline molecules is usually carried out by adopting covalent strategy [10].

A number of chalcone having reported to exhibit a broad spectrum of anti-bacterial, antifungal, antiulcer, antimalarial, antitumor, anticancer, anti-inflammatory and antitubercular activity [11, 12]. It is believe that the presence of α, β-unsaturated functional group in chalcone (–CH=CH–CO–) is responsible for anti-microbial activity, which can be altered depending upon the type of substituent present on the aromatic rings [13, 14]. It has been observed that –CO–CH=CH– linkage is less conducive to display mesomorphism as compared to –CH=N–, –COO–, –N=N linkages group because of the presence of non-linearity and angle strain arising from keto (–C=O) group [15–19]. Surprisingly, when –CO–CH=CH– linkage is linked with another linking group it becomes conductive to induces thermally stable LCs properties. Liquid crystals in the nematic group are most widely used in production of liquid crystal displays (LCD) mainly due to their unique physical properties as well as wide range of temperature. In addition, the nematic phase in which liquid crystal molecules are oriented on average along to a particular direction [20]. By applying an electric or magnetic field, the orientation of the molecules can be derived in a probable approach [21]. The chemical constitution of molecules exhibiting mesogenic property which are of great importance [22]. From the computational methods, detail study of liquid crystalline compounds with relating to similar or differ structure to exhibits phase behaviour and other optical properties [23]. In the literature studies, there are several reports of mesogenic compounds having chalcone linkage group.

Vora et al. [24] reported a homologous series of polymers containing a chalcone linkage. Soon after words Chudghar and his co-workers reported a homologous series containing on ester-chalcone linkages [25]. Yeap et al. have also synthesized mesomorphic compounds containing on ester-chalcone linkage [26]. Thaker et al. reported homologous series based on schiff base and chalconyl linking group [27]. Furthermore, they reported two novel homologous series contain schiff base and chalcone linkage group [28]. Many mesogenic homologous series contain one central linkage group were reported [29–31]. Previously, Yellamaggad et al. reported the bent-core unsymmetrical dimers in which cholesteryl ester and chalconyl moiety are present, which enhances the biaxiality and chirality of the system [32]. R.Gopalakrishnan et al. reported chalcone based single crystals, growth, and comparison of two new enone shifted chalcones and their NLO behaviour [33]. Tandel et al. studied the chain chalconyl polymers compounds to exhibiting threaded type nematic phases [34]. Doshi et al. reported chalconyl ester and chalconyl vinyl ester linkage group inbuilt between three phenyl rings and studied the effect on mesomorphism by substituted groups at terminal and lateral side [35, 36]. Shah et al. studied a nonlinear homologous series based on ester and chalcone linkage group [37]. Patel et al. reported rod type homologous series having chalconyl ester central linkage group and hexyloxy tail group [38].Gallardo and his coworkers reported polycatenar liquid crystals series based on bent shaped chalcone and cyanopyridine molecules [39]. Recently, Bhoya et al. reported chalconyl-ester linking group based homologous series [40, 41]. Furthermore, S.Kumar et al. reported chalcone based LCs compounds possessing short alkyl chain at one end and other end with variable chain lengths. These derivatives were reported to exhibit SmC, SmA and nematic phase [43].

Here, in this work, three phenyl rings based thermotropic mesogens with presence of right terminal lauryl ester tail and left side variable alkoxy group and three linking groups are synthesized and study by using POM, DSC and PXRD analysis. Furthermore, density functional theory (DFT) based HOMO, LUMO studies are carried out which supports charge transfer interactions in presently synthesized LCs compounds. Recently, our research group reported various calamitic and bent type homologous series which consisted two and three phenyl rings bonded through vinyl ester (–CH=CH–COO–) or ester (–COO–) and chalcone (–CO–CH=CH–) groups with presence of left variable side group and other part having fixed terminal substituent group [44–47].

2. Experimental

2.1. Materials

For present synthesized homologous series required materials: 4-hydroxy acetophenone, Lauric acid, 4-hydroxy benzaldehyde, 4-hydoxy benzoic acid were purchased from (S.R.L, Mumbai). N, N-dimethyl amino pyridine (DMAP) and Dicyclohexyl carbodiimide (DCC) was purchased from (Fluka Chemie, Switzerland). R-Br was purchased from (S.R.L. Chemicals, Mumbai). The solvents were dried and purified by standard method prior to use.

2.2. Measurements

Melting points were taken on Opti-Melt (Automated melting point system). The FT-IR spectra were recorded as KBr pellet on Shimadzu in the range of 3800-600 cm^{-1}. Microanalysis was performed on Perkin-Elmer PE 2400 CHN analyser. The texture images were studied on a trinocular optical polarising microscope (POM) equipped with a heating plate and digital camera. ^{1}H NMR was recorded on a 400 MHz in Bruker Advance in the range of 0.5 ppm-16 ppm using $CDCl_3$ solvent. The phase transition temperatures were measured using Shimadzu DSC-50 at heating and cooling rates of 10°C min^{-1}. Texture image of nematic phase were determined by miscibility method. Thermodynamic quantities enthalpy (ΔH) and entropy ($\Delta S = \Delta H/T$) are qualitatively discussed. For the POM measurement, the newly synthesized compound is sandwiched between glass slide and cover slip and heating and cooling rate is (2°C/min) respectively.

2.3. Synthesis of compounds in present series

2.3.1. Preparation of 4-formyl phenyl dodecanoate (1a)

4-formyl phenyl dodecanoate (1a) has been prepared by esterification of the appropriate lauric acid (2.0 mmol) and 4-hydroxy benzaldehyde (2.0 mmol), dicyclohexyl carbodiimide (DCC) (2.22 mmol) and dimethylaminopyridine (DMAP) in catalytic amount (0.2 mmol) in dry CH_2Cl_2 (DCM) (30 ml) was stirred at room temperature for 24 h. The white precipitate of DCU is obtained which was isolated by filtration and remove, while the filtrate was evaporated to dryness. The resultant crude residue was purified by column chromatography on silica gel eluting with ethyl acetate: hexane as eluent (3:2) [48].

2.3.2. Synthesis of (E)-4-(3-(4-hydroxy phenyl)-3-oxoprop-1-en-1-yl) phenyl dodecanoate (2a) (chalcone).

Chalcone (2a) was prepared by usual established method reported in literature [49]. (Brown, Yield: 61%), IR (KBr): ν_{max}/ cm^{-1} 3460 (–OH str.-bonded), 3079-2920 (–C–H str. aliphatic alkyl group), 1667 (–C=O, group), 1610 (–C=C–) aromatic, 1730 (–COO– group), 1280 (–O–CH_2– ether linkage), 962 (*trans*, alkene). Elemental analysis: calculated for $C_{27}H_{34}O_4$: Cal: 76.77; H, 8.05; found: C, 75.98; H, 7.94%.

2.3.3. Synthesis of Methyl-4-hydroxy benzoate (3a)

Equimolar proportion of p-hydroxy benzoic acid and absolute methanol shacked well in presence of two drops of concentrated H_2SO_4 and reaction mixture was refluxed for two to three hours. Then reaction mixture was dumped into ice, and allowed it to settle down. Solid white precipitate of methyl-4-hydroxy benzoate is obtained. Product was filtered, washed, dried and then purified by alcohol. Fine crystals are obtained (M.P.126°C, yield 79%) [50].

2.3.4. Synthesis of Methyl-4-n-alkoxy benzoate (3b)

Methyl-4-n-alkoxy benzoate(3b) were prepared by alkylation of Methyl-4-hydroxy benzoate (3b) with alkyl bromide (R-Br) in MeOH (C_1 to C_8) and EtOH (C_{10} to C_{18}) and reflux at 3 to 4 hrs. and then dump into ice-cold water to get final Methyl-4-n-alkoxy benzoate (3b) derivatives [50].

2.3.5. Synthesis of 4-n-alkoxy benzoic acid (3c)

4-n-alkoxy benzoic acids (3c) were prepared by dissolving comp.3b in ethanol (40 ml) and 10% aq. KOH (2 ml) was added. The resultant mixture was heated at reflux for 6 to 7 hours then cooled to room temperature, poured into ice cold water (80 ml) and then acidified with dil. HCl. The crude product obtained by filtration was recrystallized by using MeOH/DCM [51].

Comp.3C_4: IR (KBr): ν_{max}/ cm^{-1}, 3021 (C–H str.), 3301 (–OH of carboxylic group), 1650 (C=O str. of carboxylic group), 648 polymethylene group of –OC_4H_9 group. ^{1}HNMR: 0.88 (t, 3H, –OC_4H_9), 1.44 (sex, 2H, –OC_4H_9), 1.72 (q, 2H, –OC_4H_9), 4.07 (t, 2H, –OC_4H_9), 10.2 (s, 1H, –COOH group), 7.11 & 7.92 (d, 4H, first phenyl ring). Elemental analysis: $C_{11}H_{14}O_3$: Cal: C, 68.04; H, 7.21%; found: C, 67.69; H, 7.18%.

Comp.3C_8: IR (KBr): ν_{max}/ cm^{-1}, 3071 (C–H str.), 3308 (–OH of carboxylic group), 1680 (C=O str. of carboxylic group), 1710 (–COO– group), 641 polymethylene group of –OC_8H_{17} group. ^{1}HNMR: 0.88 (t, 3H, –OC_8H_{17}), 1.26-1.30 (m, 8H, –OC_8H_{17}), 1.44 (sex, 2H, –OC_8H_{17}), 1.72 (q, 2H, –OC_4H_9), 4.07 (t, 2H, –OC_8H_{17}), 10.8 (s, 1H, –COOH group), 7.12 & 7.91 (d, 4H, first phenyl ring). Elemental analysis: $C_{15}H_{22}O_3$: Cal: C, 72.00; H, 8.80%; found: C, 71.31; H, 7.68%.

2.2.6. General procedure for the synthesis of final target compounds (C)

The final target compounds (C) has been prepared by esterification of the appropriate compound (3c) (2 mmol) and compound (2a) (2 mmol), dicyclohexyl carbodiimide (DCC) (2.22 mmol) and dimethylaminopyridine (DMAP) in catalytic amount (0.2 mmol) in dry CH_2Cl_2 (DCM) (30 ml) was stirred at room temperature for 28 h. The slightly yellowish precipitate of DCU is obtained which was isolated by filtration and remove, while the filtrate was evaporated to dryness. The resultant crude residue was purified by column chromatography on silica gel eluting with ethyl acetate: hexane as eluent (3:2) [48]. The characterization data of target compounds mention in supporting information. The synthesis route of target compounds was mention in below Scheme 1.

Comp.C_1: IR (KBr): ν_{max}/ cm^{-1}, 3031 (C–H str.), 1660 (–C=O group), 1740 (–COO– group), 1280 (–O–CH_2– ether linkage), 960 (*trans* –CH=CH–). ^{1}HNMR: 0.88 (t, 2H, lauryl chain), 1.26 (m, 12H, lauryl chain), 1.30 to 1.33 (m, 4H, lauryl chain), 2.51 (t, 2H, lauryl chain), 3.71 (s, 3H, –OCH_3), 7.51 (d, 1H, $J = 15.1$ *Hz*, –CO–CH=CH–), 8.01 (d, 1H, $J = 15.1$ *Hz*, –CO–CH=CH–), 6.81 (d, 4H, first phenyl ring), 7.51 (d, 4H, second phenyl ring), 7.61

(d, 4H, third phenyl ring). Elemental analysis: $C_{35}H_{40}O_6$: Cal: C, 75.53; H, 7.19%; found: C, 75.12; H, 7.05%.

Comp.C_4: IR (KBr): ν_{max}/ cm^{-1}, 3021 (C–H str.), 1640 (–C=O group), 1730 (–COO– group), 1280 (–O–CH_2– ether linkage), 960 (*trans* –CH=CH–), 648 polymethylene group of –OC_4H_9 group. ^{1}HNMR: 0.88 (t, 6H, –OC_4H_9 and lauryl chain), 1.26 (m, 12H, lauryl chain), 1.30 to 1.33 (m, 4H, lauryl chain), 2.51 (t, 2H, lauryl chain), 4.02 (t, 2H, –OC_4H_9), 1.72 (p, 2H, –OC_4H_9), 1.41 (sex, 2H, –OC_4H_9), 7.51 (d, 1H, $J = 15.1$ *Hz*, –CO–CH=CH–), 8.01 (d, 1H, $J = 15.1$ *Hz*, –CO–CH=CH–), 6.74 (d, 4H, first phenyl ring), 7.53 (d, 4H, second phenyl ring), 7.61 (d, 4H, third phenyl ring). Elemental analysis: $C_{38}H_{46}O_6$: Cal: C, 76.25; H, 7.69%; found: C, 76.02; H, 7.48%.

Comp.C_8: IR (KBr): ν_{max}/ cm^{-1}, 303 (C–H str.), 1610 (C=O str. of carboxylic group), 1740 (–COO– group), 1280(–O–CH_2– ether linkage), 960 (*trans*, –CH=CH–), 641 polymethylene group of –OC_8H_{17} group. ^{1}HNMR: 0.88 (t, 6H, –OC_8H_{17} and lauryl chain), 1.26-1.30 (m, 24H, –OC_8H_{17} and lauryl chain), 1.43 (p, 2H, –OC_8H_{17}), 1.74 (p, 2H, –OC_8H_{17}), 4.01 (t, 2H, –OC_8H_{17}), 2.52 (t, 2H, lauryl chain), 7.52 (d, 1H, $J = 15.1$ *Hz*, –CO–CH=CH–), 8.01 (d, 1H, $J = 15.1$ *Hz*, –CO–CH=CH–), 6.71 (d, 4H, first phenyl ring), 7.56 (d, 4H, second phenyl ring), 7.60 (d, 4H, third phenyl ring). Elemental analysis: $C_{42}H_{54}O_6$: Cal: C, 77.06; H, 8.25%; found: C, 76.91; H, 8.21%.

2.2.7. Reaction and scheme

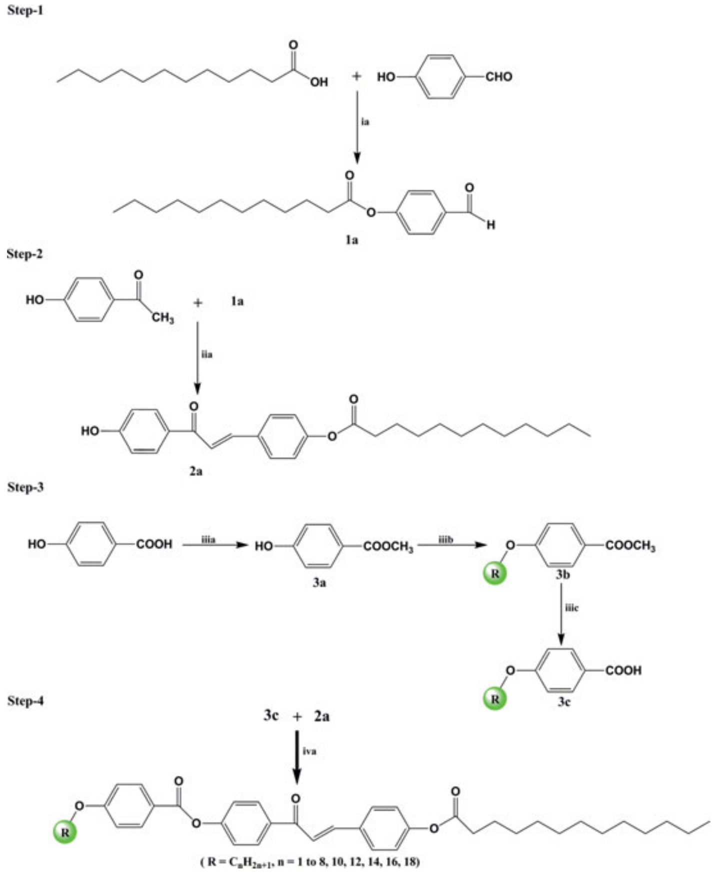

Scheme 1(ia). DCC/DMAP, DCM, 48 hr. stirring (rt); (iia) KOH, EtOH, 24 hr. stirring (rt); (iiia) MeOH, conc.H_2SO_4, 1 hr. reflux; (iiib) R-Br, KOH, MeOH, 2 to 3 hr. reflux; (iiic) KOH, EtOH, 2 hr. reflux; (iva) DCC/DMAP, DCM, 48 hr. stirring (rt).

3. Result and discussion

3.1. Mesomorphic behaviour study

Here in present investigation, we have synthesized newly liquid crystalline compounds having three linking unit joint via three phenyl rings from small alkyl chain (C_1) to higher alkyl chain (C_{18}) at left end side chain with fixed lauryl tail group at right terminal side in present series. A newly ester-chalcone-ester linking group based homologous series synthesised from condensation of 4-n-alkoxy benzoic acid (3c) and (*E*)-4-(3-(4-hydroxy phenyl)-3-oxoprop-1-en-1-yl) phenyl dodecanoate (2a) (chalcone) is synthesized and evaluated their LC behaviour. The thermotropic mesophase behaviour of all newly synthesised compounds was primarily investigated by polarising optical microscope (POM). The exact temperature of phase transition and associated enthalpy values were determined by differential scanning calorimetry (DSC) analysis. The presence of SmC phase is confirmed by XRD technique at transition temperature. We have totally prepared thirteen compounds in present series from lower member to higher member, out of thirteen compounds, comp.(C_3 to C_6) shows only enantiotropic SmC phase, comp. (C_7 to C_{12}) shows enantiotropic smectic C and nematic phase while comp.(C_{14} to C_{18}) display only nematic phase with wide range of temperature.

3.1.1. POM study

We have studied the effect of changing variable aliphatic alkoxy side chain on mesogenic property of liquid crystalline compounds. Here, in present article, we have synthesized three phenyl ring based calamitic rod-shaped mesogens having two ester (−COO−) and chalcone (−CH=CH−CO−) group at central part with presence of terminal substituent on both sides. The transition temperature of present series is listed in Table 1. As seen in Table 1, compounds C_1 to C_2 shows non liquid crystalline nature, The nonmesomorphicity of comp.C_1 to C_2 is attributed to their high crystallising tendency which arises due to low magnitudes of dispersion forces and low dipole-dipole interaction which results into unsuitable magnitudes of anisotropic forces of intermolecular end to end or lateral attractions as a consequence of unfavorable combined effects of molecular rigidity and flexibility [52]. While comp. C_3 to C_6 display only smectic C phase on both heating and cooling condition, comp. C_7 to C_{18} shows nematic phase. Mesophase formation was found to be dependent on the number, position

Table 1. Transition temperature in °C by POM.

		Transition temperatures in ^{0}C						
Sr.no	R = n-alkyl group	Cr-I	Cr-SmC		SmC-N		SmC/N-I	
1	C_1	215.0	—	—	—	—	—	—
2	C^2	212.0	—	—	—	—	—	—
3	C_3	·	173.0	·	—	—	208.0	·
4	C_4	·	169.0	·	—	—	192.0	·
5	C_5	·	166.0	·	—	—	189.0	·
6	C_6	·	168.0	·	—	—	188.0	·
7	C_7	·	156.0	·	172.0	·	181.0	·
8	C_8	·	152.0	·	168.0	·	184.0	·
9	C_{10}	·	143.0	·	163.0	·	180.0	·
10	C_{12}	·	138.0	·	159.0	·	177.0	·
11	C_{14}	·	—	—	136.0	·	167.0	·
12	C_{16}	·	—	—	127.0	·	162.0	·
13	C_{18}	·	—	—	125.0	·	158.0	·

(Cr–I=Crystal to isotropic phase; Cr-SmC = crystal to smectic C phase; SmC-N = smectic C to nematic phase; N-I = nematic to isotropic phase).

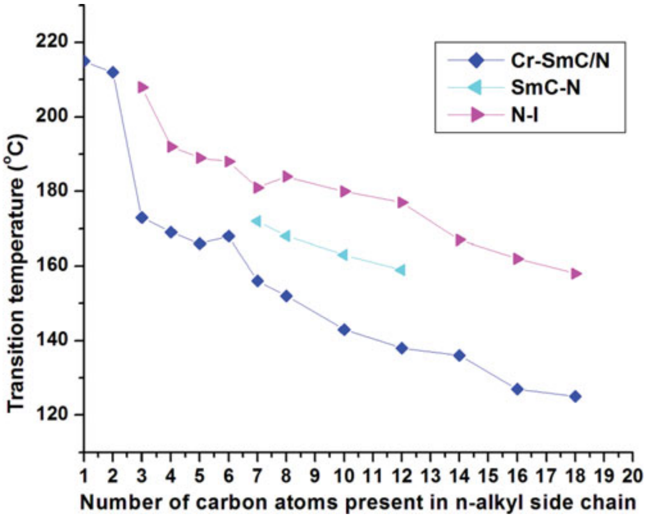

Figure 1. Phase diagram of present series.

and the molecular length of the side alkyl chain which increases the flexibility of molecules attached to the alkoxy side group (-OR). As shown in Table 1, lower member compounds of present series shows wide temperature range of mesophase as compare to higher members.

The phase diagram of present series is shown in Figure 1 which indicates the phase behaviour of Cr-SmC/N, SmC-N and N-I transition curve. It can be seen that, as series increases from lower homologue (C_1) to higher homologue (C_{18}), the transition temperature gradually is decreases. Cr-SmC/N phase transition curve exhibit a smooth falling tendency from comp. C_1 to C_5 and formerly increases at comp.C_6, this is due to the presence of odd-even parity of carbon present in n-alkyl side chain and from comp.C_6, it continued to exhibit descending tendency upto last homologue (C_{18}). Odd-even effect is present at comp. (C_5-C_6) and comp. (C_6-C_7) in Cr-SmC/N transition curve. SmC-N transition curve shows descending tendency without exhibiting any odd-even effect. N-I transition curve shows falling tendency upto comp.C_7 and then slightly increase at comp.C_8 and continued to showing falling tendency upto last homologue. The decreasing tendency in melting and clearing temperature could be due to the lowering the vander waals interactions between aromatic phenyl cores and higher degree of flexibility due to presence of long alkyl chain in alkoxy group at left terminal part and also the presence of lauryl ester at right tail side.

3.1.2. Textural study

The crystalline compounds placed on clear glass slide sheltered by coverslip were heated to the isotropic state and heating and cooling rate is (2°C/min) respectively and observing mesophase texture image. Microphotographs of the textures observed for compounds C_{10} and C_4 are depicted in Figure 2. Comp.C_{10} shows broken fan like texture image of smectic C phase at 143.0°C on cooling condition. Comp. C_4 shows needle type texture image of smectic C phase at 169.0°C on cooling condition. The texture pattern is also being seen in heating condition. It can be noted that, presence of mesophase in present series is enantiotropical type.

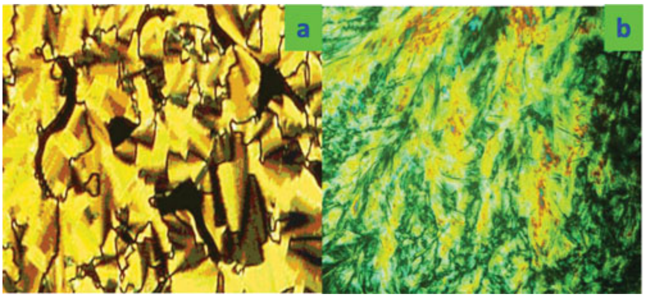

Figure 2. Optical photomicrographs on cooling; (a) smectic C (comp.C_{10}) at 143°C; (b) smectic C (comp.C_4) at 169°C.

3.1.2. Comparative study

Figure 3 indicates the geometrical optimized structure of present series which is calamitic rod type, consequently, the phenyl rings of the core are connected through ester, chalcone and ester linking units while lauryl ester and alkoxy chains are positioned at terminal locations. By varying the length of the left alkoxy chain from C_1 to C_8, C_{10}, C_{12}, C_{14}, C_{16}, C_{18}, eleven mesogens are prepared. The presence of polar flexible methylene part in variable alkoxy chain and also presence of decanoyl ester or lauryl ester at right terminal part increases the polarity and flexibility of molecule to induce mesomorphism. Presence of middle chalcone group is become conductive in presence of two ester group to display LCs property. Figure 4 shows the planar structure of selected two compounds C_4 and C_{14} along with carbon numbers and the geometry optimized structure from DFT. The overall molecular length of comp.C_{14} is higher as compare to comp.C_4 while the bond angle at linking group side is similar in both of the compounds. The dipole moment of comp.C_4 is slightly higher as compare to comp.C_{14}. Comp.C_{14} shows only nematic phase due to the presence of long side chain in both the sides to becomes more flexible and absence of lamellar packing arrangement of molecules while in comp.C_4, due to the short alkyl spacer at one end and presence of lamellar packing order in molecules to induce smectic C phase and on further heating it transform into isotropic state without displaying any nematic type textural pattern on heating and cooling condition.

3.1.3. Frontier molecular orbital (FMO) distribution

The calculated frontier molecular orbital (FMO) distributions of comp.C_4, comp.C_{10} and comp.C_{18} are presented in Figure 5, 6, 7. The HOMO/LUMO gap in comp.C_4 is lower as

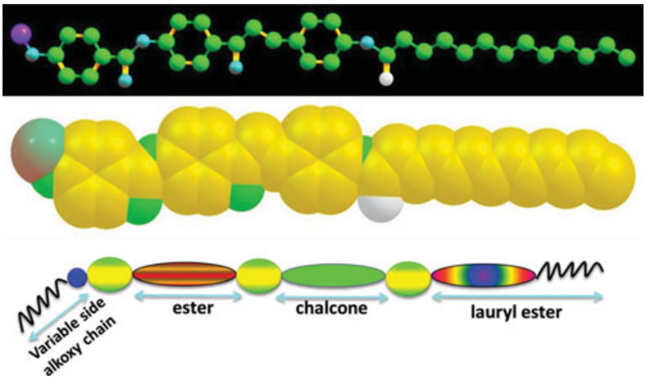

Figure 3. Space-filing diagram and geometrical shape of present series.

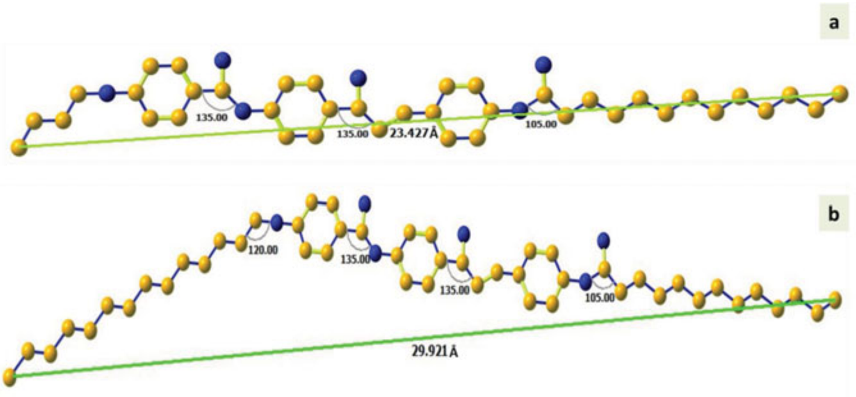

Figure 4. Expected molecular configuration with length and bond angle of (a) comp.C_4; (b) comp.C_{14} by MM_2 method.

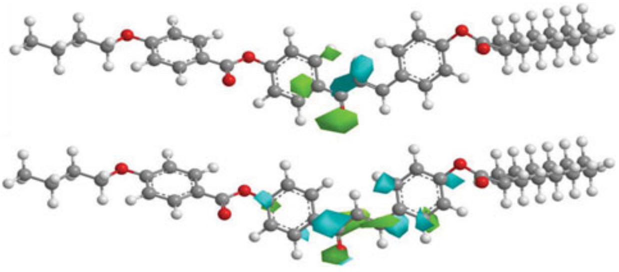

Figure 5. FMO distribution of comp.C_4.

compare to comp.C_{10} and comp.C_{18} due to the presence of short alkyl spacer at one terminal end. In Figure 5, A close examination of these orbitals reveal that the HOMO is predominantly localized on the second phenyl and chalcone linking unit while the LUMO is mostly concentrated on both phenyl benzoate and chalcone unit; lauryl ester and butoxy part in both terminal side does not have any significant influence on the HOMO and LUMO orbitals. In

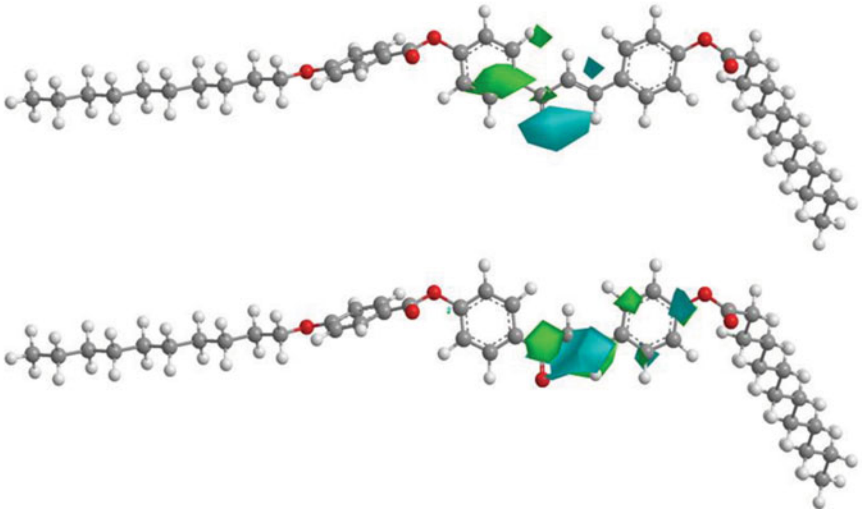

Figure 6. FMO distribution of comp.$C_{10.}$

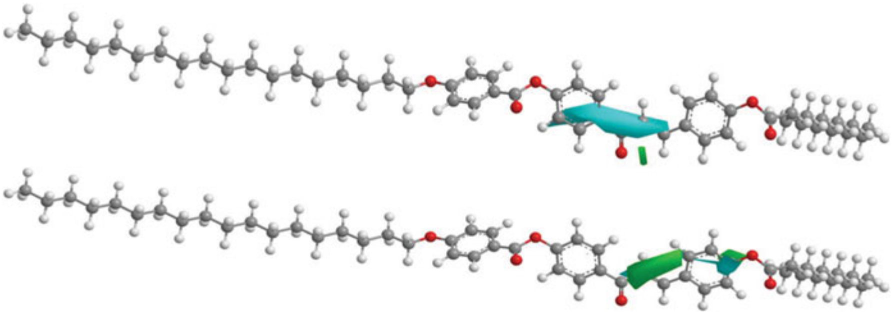

Figure 7. FMO distribution of comp.$C_{18.}$

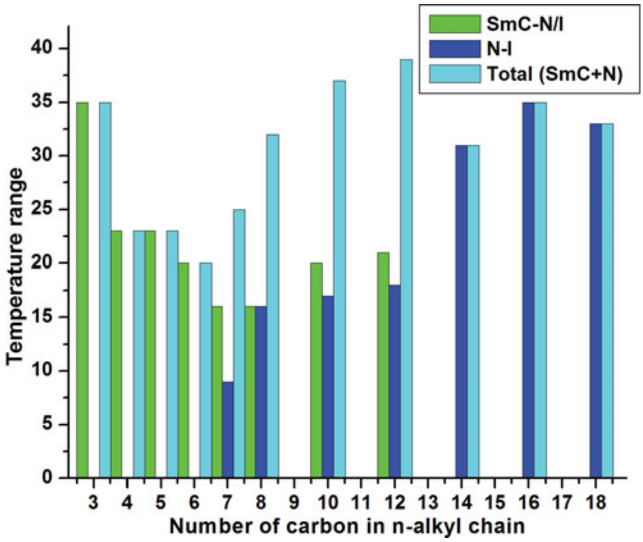

Figure 8. Temperature range of phase transition in series.

Figure 6, HOMO is localized on the second phenyl and chalcone unit while LUMO is localized on chalcone unit and third phenyl ring. From the Figure 7, it can be seen that the distribution of HOMO and LUMO are contrasted as increasing in alkoxy side chain at left tail part. Thus, it can be concluded that the electronic properties of present synthesized compounds could have originated from the phenylic-chalcone group rather than other linking unit [53].

3.1.4. Thermal stability and temperature range

Thermal stability of present novel synthesised series is listed in Table 2. From the Table 2, presently series display smectic C and nematic phase with good thermal stability. SmC-I transition curve shows higher thermal stability as compare to other phase transition. Mesophase commences from C_3 homologue in present series. Temperature range of present

Table 2. Average thermal stability in °C.

Series	Series
SmC-I	194.25 (C_3-C_6)
SmC-N	165.53 (C_7-C_{12})
Cr-SmC	158.12 (C_3-C_{12})
N-I	172.71 (C_7-C_{18})

(SmC-I = smectic C to isotropic; SmC-N = smectic C to nematic; Cr-SmC = solid to smectic C; N-I = nematic to isotropic).

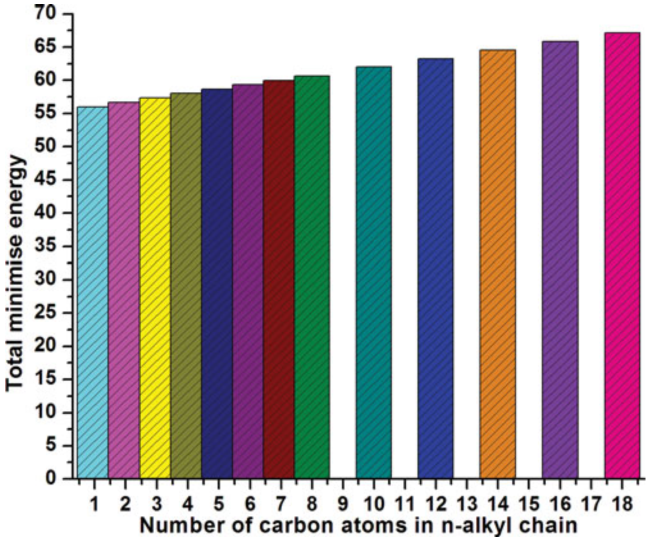

Figure 9. Total minimizes energy of present series.

series is shown in Figure 8. From careful observation of Figure 8, we have noted that the temperature range of lower member and higher member is higher as compare to middle member of present series. Comp.C_{10} and comp.C_{12} shows good total thermal stability as compare to other member of present series. We have compared the total minimize energy and dipole/dipole interactions value for present thirteen compounds in series which is mention in Figure 9 and Figure 10 respectively. From Figure 9, it can be noted that, as number of alkyl chain in alkoxy group increase the value of total energy minimize is also increases. As dipole/dipole interaction is in decreasing order from comp.C_1 to C_{10} except comp.C_5, C_7 and higher homologoues of series.

Figure 11 represents the proposed mechanism to indicate the arrangement of lamellar packing in molecules to shows SmC and on further heating transform into nematic phase.

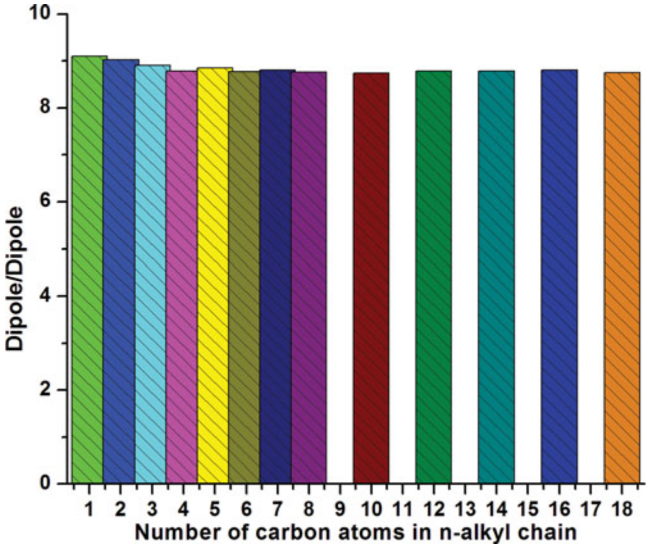

Figure 10. Dipole/dipole interaction in present series.

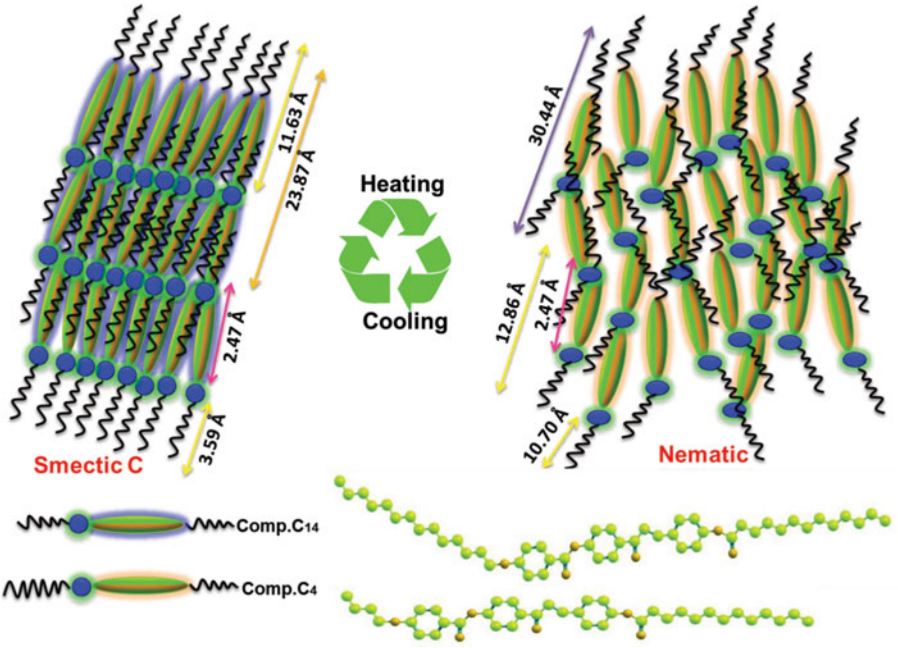

Figure 11. Propose mechanism of present series.

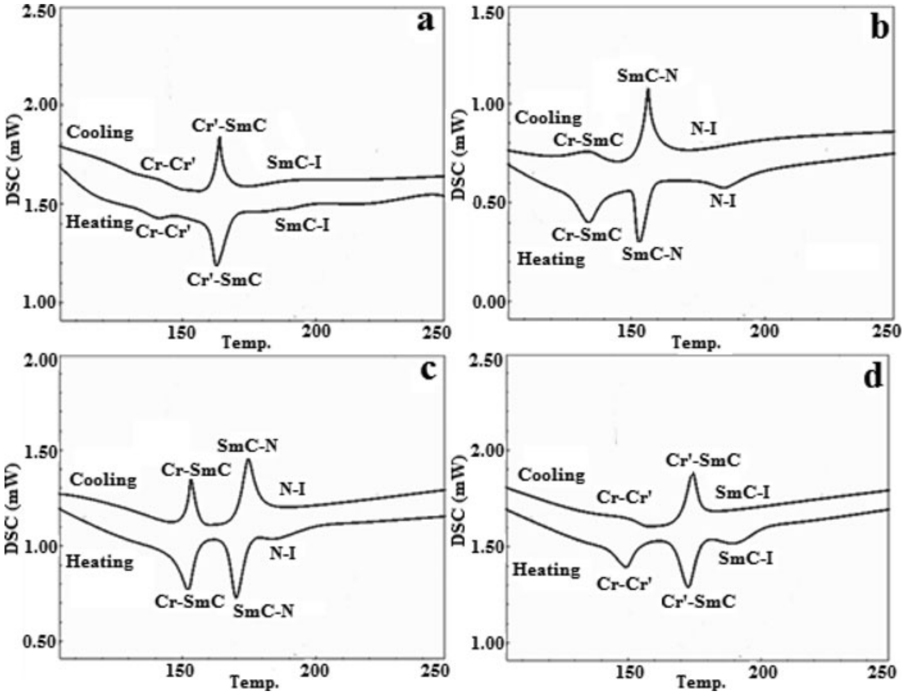

Figure 12. DSC thermograms of compound (a) comp.C_5; (b) comp.C_{12}; (c) comp.C_8; (d) comp.C_6 on heating and cooling cycles.

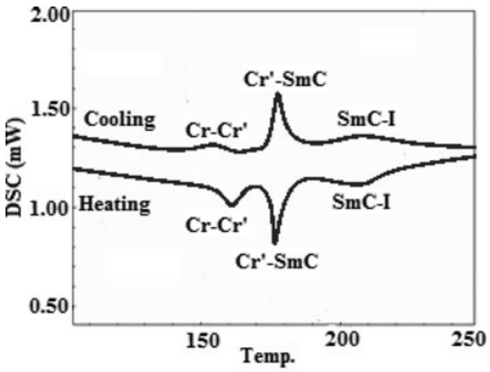

Figure 13. DSC thermograms of compound of comp.C_{18} on heating and cooling cycles.

In Figure 11, we have compare the structural arrangement of comp.C_4 and C_{14} in which comp.C_4 shows only smectic C phase while comp.C_{14} display only nematic phase. Both of the compounds show mesophase on heating and cooling condition. The molecular length of comp.C_{14} is higher as compare to comp.C_4 due to the presence of long alkyl chain which increases the flexibility and polarity of molecule and does not exits any lamellar packing type arrangement in molecules to exhibit smectic phase.

3.2. DSC analysis

The phase transition temperatures and enthalpies were measured by carrying out DSC thermal analysis. All compounds are thermally stable as confirmed by the reproducibility of thermograms on several heating and cooling cycles. In Figure 12, comp.C_5 exhibits one significant endothermic peak at 162.81°C in heating cycle, which correspondence to the presence of crystal to smectic C phase and on cooling condition, it appears at 163.24°C which reveals with POM result. Comp. C_{12} shows three endothermic peak at 135.21°C, 154.27°C and 182.36°C on heating cycle corresponding to Cr-SmC, SmC-N and N-I phase transition, while on cooling cycle, it again appears at 138.02°C and 156.72°C which was further confirmed by POM analysis which suggest that the mesophase appeared is SmC

Table 3. Transition temperature (°C) and enthalpy (J g^{-1}) and entropy change (J $g^{-1}k^{-1}$) by DSC measurement.

Comp.	Transition	Heating scan(°C)	Cooling scan(°C)	ΔH (Jg^{-1})	ΔH (Jg^{-1})	ΔS (J $g^{-1}k^{-1}$)	ΔS (J $g^{-1}k^{-1}$)
C_5	**Cr-Cr′**	140.02	138.12	6.82	2.42	0.0182	0.0064
	Cr′-SmC	162.81	163.24	23.94	13.54	0.0576	0.0326
	SmC-I	188.18	—	2.21	—	0.0051	—
C_{12}	**Cr-SmC**	135.21	138.02	14.81	10.92	0.0357	0.0263
	SmC-N	154.27	156.72	1.95	2.63	0.0045	0.0060
	N-I	182.36	—	2.42	—	0.0055	—
C_8	**Cr-SmC**	150.92	152.32	28.73	21.82	0.0764	0.0570
	SmC-N	169.01	175.27	3.74	6.43	0.0095	0.0163
	N-I	180.61	—	1.52	—	0.0037	—
C_6	**Cr-Cr′**	149.86	148.18	3.32	1.42	0.0094	0.0040
	Cr′-SmC	171.08	172.63	30.21	23.75	0.0777	0.0613
	SmC-I	185.35	—	2.21	1.04	0.0053	0.0025
C_3	**Cr-Cr′**	161.08	150.26	1.67	1.43	0.0044	0.0039
	Cr′-SmC	175.95	176.08	12.42	10.43	0.0291	0.0244
	SmC-I	203.01	—	1.43	—	0.0032	—

(Cr-Cr′ = solid to solid crystal; Cr′-SmC = solid to SmC; SmC-N = SmC to nematic; N-I = nematic to isotropic).

and nematic type. Comp. C_8 shows two endothermic peaks at 150.92°C and 169.01°C on heating condition and again reappears at 152.32°C and 175.27°C on cooling condition which confirm the results obtain by POM study. Comp.C_6 exhibits endothermic peaks at 149.88°C, 171.08°C and 185.35°C on heating cycle while on cooling cycle, again these exothermic peaks traced at 148.18°C and 172.63°C confirm the presence of solid to solid, solid to smectic C and smectic C to isotropic transition. In Figure 13, Comp.C_3 shows endothermic peaks at 161.08°C, 175.95°C and 203.01°C in heating condition while on cooling condition; it appears at 150.26°C and 176.08°C which reveals with POM result. The phase transition temperatures, enthalpy and entropy values for the present synthesized series are summarized in Table 3.

4. Conclusion

A new calamitic chalconyl ester derived LCs compounds based on three phenyl rings as rigid core possessing three linking unit having lauryl side group at right end and other end with variable alkyl chain length in alkoxy group (-OR). The liquid crystalline properties of the synthesized mesogens are carried out by POM and DSC methods which revealed the occurrence of enantiotropic nematic as well as addition of smectic C phase in comp. (C_7 to C_{12}). The lower member comp. (C_1, C_2) shows non liquid crystalline nature due to the presence of short alkyl spacer in right end alkoxy group. Comp. (C_3 to C_6) shows only enantiotropical smectic C phase while comp. (C_7 to C_{12}) shows smectic C and nematic phase with higher value of temperature range and thermal stability. Comp. (C_{14} to C_{18}) shows nematic phase without displaying any smectic phase on heating and cooling condition. The group efficiency order derived on the basis of (a) mesophase thermal stability, (b) early or late commencement of mesophase, (c) Temperature range of mesophase. The HOMO-LUMO calculations indicated the intermolecular charge transfer interactions and revealed the electronic properties of present synthesized newly compounds were originated from second and third phenyl to chalcone moiety.

Acknowledgement

Authors acknowledge thanks to Dr. R. R. Shah, principal and management of K. K. Shah Jarodwala Maninagar Science College, Ahmedabad. Authors are also thankful to NFDD Centre for providing analytical and spectral services.

References

[1] Macros, M., Omenat, A., Serrano, J. L., & Ezcurra, A. (1992). *Adv. Mater.*, 4, 285.
[2] Hird, M., Toyne, K. J., & Gray, G. W. (1993). *Liq. Cryst.*, 14, 741.
[3] Hird, M., Toyne, K. J., Gray, G. W., Day, S. E., & Mc Donnell, D. G. (1993). *Liq. Cryst.*, 15, 123.
[4] Hird, M. (2011). *Liq. Cryst.*, 38, 11.
[5] Teucher, I., Paleos, C. M., & Labes, M. M. (1970). *Mol. Cryst. Liq. Cryst.*, 11, 187.
[6] Kim, W. S., Elston, S. J., & Raynes, F. P. (2008). *Display.*, 29, 458.
[7] Hertz, E., Lavorel, B., & Faucher, O. (2011). *Nat. Photon.*, 5,783.
[8] Vora, R. A., & Dixit, N. (1980). *Mol. Cryst. Liq. Cryst.*, 59, 63.
[9] Glendenning, M. E., Goodby, J. W., Hird, M., Jones, J. C., Toyne, K. J., Slaney, A. J., & Minter, V. (1999). *Mol. Cryst. Liq. Cryst.*, 332, 321.
[10] Thaker, B. T., & Kanojiya, J. B. (2011). *Liq. Cryst.*, 38, 1035.
[11] Sashidhara, K. V., Rao, K. B., Kushwaha, P., Modukuri, R. K., Singh, P., Soni, I., Shukla, P. K., Chopra, S., & Pasupuleti, M. (2015). *ACS Med. Chem. Lett.*, 6, 806.

[12] Qian, Y., Zhang, H. J., Zhang, H., Xu, H., Zhao, J., & Zhu, H. L. (2010). *Bioorg. Med. Chem.*, 18, 4991.

[13] Nielsen, S. F., Larsen, M., Boesen, T., Schonning, K., & Kromann, H. (2005). *J. Med. Chem.*, 48,2667.

[14] (a) Bozic, D. D., Milenkovic, M., Ivkovic, B., Cirkovic, I. (2014). *Indian J. Med Res.*, 140(1),130; (b) Doan, T. N., Tran, D. T. (2011). *Pharmacol. Pharm.*, 2, 282; (c) Ngyyen, H., Zanna, T., & Duboisj, C. (1979). *Mol. Cryst. Liq. Cryst.*, 53, 43.

[15] Pelzl, G., Diele, W. S., & Weissflog, W. (1999). *Adv. Mater.*, 11(9), 707.

[16] Dave, J. S., Menon, M. R., & Patel, P. R. (2001). *Mol. Cryst. Liq. Cryst.*, *364*, 575.

[17] Vora, R. A., Patel, D. N. (1983). *Mol. Cryst. Liq. Cryst.*, 103, 127.

[18] Dave, J. S., Upasani, C. B., & Patel, P. D. (2010). *Mol. Cryst. Liq. Cryst.*, 533, 73.

[19] (a) Kang, Y. S., Kim, H., & Zin, W. C. (2001). *Liq. Cryst.*, 28, 709; (b) Kato, T., & Frechet, J. M. J. (1989). *J. Am. Chem. Soc.*, 111, 8533.

[20] Gray, G. W. (1962). *Molecular Structure and the Properties of Liquid Crystals*, Academic Press: London and New York.

[21] Madsen, L. A., Dingemans, T. J., Nakata, M., & Samulski, E. T. (2004). *Phys. Rev. Lett.*, 92(14), 145505.

[22] Kopp, V. I., Fan, B., Vithana, H., & Genack, H. K. M. (1998). *Opt. Lett.*, 23, 1707.

[23] (a) Gray, G. W., Harrison, K. J., & Nash, J. A. (1973). *Electron. Lett.*, 9(6), 130; (b) Kelker, H., & Scheurle, B. (1969). *Angew. Chem. Int. Ed.*, 8(11), 884.

[24] Oliveira, B. F., Avelino, P. P., Moraes, F., & Oliveira, J. C. R. E. (2010). *Phys. Rev. E.*, 82, 041707.

[25] Vora, R. A., & Sheth, K. A. (1987). *Presented at the International Conference of Liquid Crystals Polymers*, Bordeaux, France.

[26] Chudgar, N. K., & Shah, S. N. (1989). *Liq. Cryst.*, 4(6), 661.

[27] Yeap, G. Y., Susanti, I., Teoh, B. S., Mahmood, W. A. K., & Harrison, W. T. A. (2005). *Mol. Cryst. Liq. Cryst.*, 442, 133.

[28] Thaker, B. T., Patel, P. H., Vasadiya, A. D., & Kanojiya, J. B. (2009). *Mol. Cryst. Liq. Cryst.*, 515, 135.

[29] (a) Thaker, B. T., & Kanojiya, J. B. (2011). *Mol.Cryst.Liq.Cryst.*, 542, 84; (b) Thaker, B. T., Patel, D. M., & Kanojiya, J. B. (2009). *Mol. Cryst. Liq. Cryst.*, 509, 145.

[30] (a) Sharma, V. S., Vekariya, R. H., Sharma, A. S., & Patel, R. B. (2017). *Liq. Cryst. Today*., 26(3), 46; (b) Sharma, V. S., Jain, B. B., & Patel, R. B. (2016). *Mol. Cryst. Liq. Cryst.*, 638, 68;

[31] (a) Sharma, V. S., & Patel, R. B. (2016). *Mol. Cryst. Liq. Cryst.*, 637, 19; (b) Sharma, V. S., & Patel, R. B. (2016). *WSN.*, 54, 240.

[32] Solanki, R., Sharma, V., & Patel, R. (2016). *Mol. Cryst. Liq. Cryst.*, 631, 107.

[33] Yelamaggad, C. V., Mathews, M., Negamani, A., S. Rao., Prasad, S. K., Findeisen, S., & Weissflog, W. (2007). *J. Mater. Chem.*, 17, 284.

[34] Ramkumar, V., Anandhi, S., Kannan, P., & Gopalakrishnan, R. (2013). *Cryst. Eng. Comm.*, 15, 2438.

[54] Tandel, R. C., Gohil, J., & Patel, N. K. (2012). *Res. J. Recent Sci.*, 1,122.

[36] (a) Suthar, D. M., & Doshi, A. V. (2013). *Mol. Cryst. Liq. Cryst.*, 575, 76; (b) Chauhan, H. N., & Doshi, A. V. (2013). *Mol. Cryst. Liq. Cryst.*, 570, 92.

[37] Chaudhari, R. P., Chauhan, M. L., & Doshi, A. V. (2013). *Mol. Cryst. Liq. Cryst.*, 575, 88.

[38] Patel, P. K., & Shah, R. R. (2017). *Mol. Cryst. Liq. Cryst.*, 643, 168.

[39] Pandya, S. H., & Patel, V. R. (2017). *Mol. Cryst. Liq. Cryst.*, 642, 1.

[40] Coelho, R. L., Westphal, E., Mezalira, D. Z., & Gallardo, H. (2016). *Liq. Cryst.*, 44, 405.

[41] (a) Namera, D. L., Ranch, A. R., Bhoya, U. C. (2017). *Mol. Cryst. Liq. Cryst.*,643, 233; (b) Rakhasia, P. K., Ranchchh, A. R., Bhoya, U. C. (2017). *Mol. Cryst. Liq. Cryst.*, 643, 159.

[42] Rakhasia, P. K., & Bhoya, U. C. (2016). *Mol. Cryst. Liq. Cryst.*, 625, 55.

[43] Rakhasia, P. K., Bhola, G. N., & Bhoya, U. C. (2016). *Mol. Cryst. Liq. Cryst.*, 623, 81.

[44] Srinivasa, H. T., & Kumar, S. (2017). *Liq. Cryst.*, 44, 1.

[45] (a) Solanki, R. B., Sharma, V. S., & Patel, R. B. (2017). *Mol. Cryst. Liq. Cryst.*, 643, 216; (b) Sharma, V. S., & Patel, R. B. (2017). *Mol. Cryst. Liq. Cryst.*, 643, 241; (c) Sharma, V. S., & Patel, R. B. (2017). *Mol. Cryst. Liq. Cryst.*, 643, 13; (d) Sharma, V. S., & Patel, R. B. (2017). *Mol. Cryst. Liq. Cryst.*, 643,141.

[46] (a) Sharma, V. S., & Patel, R. B. (2017). *Mol. Cryst. Liq. Cryst.*, 643, 52; (b) Sharma, V. S., & Patel, R. B. (2017). *Mol. Cryst. Liq. Cryst.*, 643, 62.

[47] (a) Sharma, V. S., & Patel, R. B. (2017). *Mol. Cryst. Liq. Cryst.*, 643, 129; (b) Sharma, V. S., & Patel, R. B. (2017). *Mol. Cryst. Liq. Cryst.*, 643, 178.

[48] (a) Sharma, V. S., & Patel, R. B. (2016). *Mol. Cryst. Liq. Cryst.*, 630, 58; (b) Sharma, V. S., & Patel, R. B. (2017). *Mol. Cryst. Liq. Cryst.*, 643, 40; (c) Sharma, V. S., & Patel, R. B. (2016). *Mol. Cryst. Liq. Cryst.*, 630, 162; (d) Sharma, V. S., & Patel, R. B. (2016). *Mol.Cryst.Liq.Cryst.*, 633, 80; (e) Sharma, V. S., Solanki, R. B., Patel, P. K., & Patel, R. B. (2016). *Mol.Cryst.Liq.Cryst.*, 625, 137.

[49] Lutfor, M. R., Yusoff, M. M., Hegde, G., Fazli, M. N., Malek, A., & Samah, N. A. (2013). *Mol. Cryst. Liq. Cryst.*, 587, 41–53.

[50] (a) Solanki, R. B., & Patel, R. B. (2015). *ILCPA.*, 60, 152; (b) Sharma, V. S., & Patel, R. B. (2015). *ILCPA.*, 59,115.

[51] Jain, B. B., Jadeja, U. H., Sharma, V. S., Patel, R. B. (2016). *Mol. Cryst. Liq. Cryst.*, 625, 146.

[52] Prasad, V. (2001). *Liq. Cryst.*, 28,145.

[53] Gray, G. W. (1962). *Molecular Structure and Properties of Liquid Crystals*, Academic Press: London and New York.

[54] Reddy, M. G., Varathan, E., Lobo, N. P., Shanmugam, E., Narasinhaswamy, T., & Mandal, A. B. (2015). *J. Phys. Chem. C.*, 119(17), 9477.